# Analyzing Reachability of Linear Dynamic Systems with Parametric Uncertainties

Matthias Althoff (✉), Bruce H. Krogh, and Olaf Stursberg

**Abstract** As an important approach to analyzing safety of a dynamic system, this paper considers the task of computing overapproximations of reachable sets, i.e. the set of states which is reachable from a given initial set of states. The class of systems under investigation are linear, time-invariant systems with parametric uncertainties and uncertain but bounded input. The possible set of system matrices due to uncertain parameters is represented by matrix zonotopes and interval matrices – computational techniques for both representations are presented. The reachable set is represented by zonotopes, which makes it possible to apply the approach to systems of 100 continuous state variables with computation times of a few minutes. This is demonstrated for randomized examples as well as a transmission line example.

## 1 Introduction

Reachability analysis deals with the problem of finding the set of states that a system can reach when starting from a specified set of initial states in finite or infinite time. One of the main purposes of reachability analysis is to demonstrate the safe execution of a system by proving that the system does not reach any unsafe state. This is illustrated for a two-dimensional example with states $x_1$, $x_2$ in Fig. 1. Besides the safety verification problem, reachability analysis is a useful tool for robustness analysis [1], abstraction of hybrid systems [2], and state-bounding observers [3].

Matthias Althoff
Carnegie Mellon University, 5000 Forbes Ave, Pittsburgh, PA e-mail: malthoff@ece.cmu.edu

Bruce H. Krogh
Carnegie Mellon University, 5000 Forbes Ave, Pittsburgh, PA e-mail: krogh@ece.cmu.edu

Olaf Stursberg
University of Kassel, Control and System Theory (FB16), Wilhelmshoeher Allee 73, 34121 Kassel, Germany. e-mail: stursberg@uni-kassel.de

In this work, an efficient algorithm for computing reachable sets of continuous-time linear systems with uncertain inputs/disturbances and constant but uncertain parameters is presented. One advantage of the proposed method is that the computational complexity is moderate in terms of the system dimension. As shown by earlier work, the reachability algorithm for linear systems can be extended to the analysis of nonlinear systems [4] and hybrid systems [5]. Thus, the reachability analysis of linear systems can be seen as a basic module for the reachability analysis of more complicated system classes.
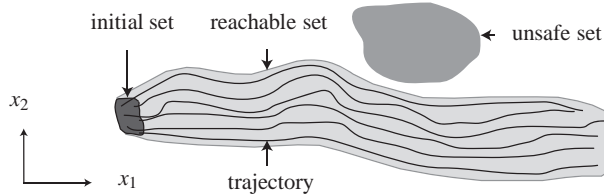


**Fig. 1** An empty intersection of (an overapproximation of) the reachable set with an unsafe set of states verifies system safety

For systems with derivative bounds $\dot{\mathbf{x}} \in P$, where $\mathbf{x} \in \mathbb{R}^n$ and $P$ is a bounded convex polyhedron (polytope) in $\mathbb{R}^n$, the reachable set can be represented by polyhedra [6]. Reachable sets of such systems can be used as a basis for the reachability analysis of linear or even more complex systems, such as nonlinear and hybrid systems [7, 8].

Other work deals directly with linear systems $\dot{\mathbf{x}}(t) = \mathbf{A}\mathbf{x}(t) + \mathbf{u}(t)$, where $\mathbf{x} \in \mathbb{R}^n$, $\mathbf{u} \in U \subset \mathbb{R}^n$, $\mathbf{A} \in \mathbb{R}^{n \times n}$. Exact reachable sets of linear systems can only be obtained in special cases; in general one has to compute overapproximations to perform system verification [9]. Approaches to this class of systems can be classified by the geometric representation used for the reachable sets: polytopes [10], ellipsoids [11], oriented rectangular hulls [12], zonotopes [13, 14], or level sets [15]. Support functions [16] unify these methods, except of the use of level sets. If uncertain parameters are considered, most existing algorithms are based on interval methods and multidimensional intervals (hyperrectangles) to represent reachable sets [17–19]. Similar techniques are used for validated integration methods of ordinary differential equations, which are typically applied to smaller uncertainties in the initial states [20–22].

Besides the mentioned techniques that are based on guaranteed set integration, for which an overview can be found in [23], one can verify the safety of a system with barrier certificates [24] or simulation based techniques, e.g. [25, 26].

Previous work addressed the computation of reachable sets of linear systems with uncertain parameters [27]. Recently, this approach has been extended to linear systems with time-varying uncertain parameters [28]. In these works, the reachable sets are represented by zonotopes, which offer a more general representation compared to multidimensional intervals, which are typically used for this class of problems. Zonotopes are also a more efficient alternative to arbitrary polytopes for reachability

analysis of linear systems [14]. The novelties for the follow-up work presented here
are:

- Improved computational techniques: Dependencies between the elements of state transition matrices due to common parameters are considered when computing with matrix zonotopes.
- A norm bound for the computation of matrix exponential sets is derived.
- Performance evaluations of methods for computing matrix exponential sets are conducted.
- Properties of a new transmission line example are verified.

This book chapter is organized as follows. In Section 2, the problem of computing reachable sets is introduced, and a brief description of the used algorithmic procedure is given. The formulas for computing reachable sets of linear systems under uncertain initial states, parameters, and inputs are derived in Section 3. These formulas are based on the set of possible state transition matrices, of which the computation is described in Section 4. The usefulness of the presented approach is demonstrated for a transmission line example, and randomly generated examples in Section 5.

## 2 Problem Formulation

We consider time-invariant linear systems of the form

$$\dot{\mathbf{x}}(t) = \mathbf{A}\,\mathbf{x}(t) + \mathbf{u}(t), \quad \mathbf{A} \in \mathscr{A}, \mathbf{u}(\cdot) \in \mathscr{U}_{[0,t_f]}, \mathbf{x}(0) \in \mathscr{X}_0, t \in [0,t_f],$$

where $\mathbf{u}(t) : \mathbb{R}^+ \to \mathbb{R}^n$ is an input function over time, $\mathscr{A}$ is the set of system matrices $\mathbf{A}$, $\mathscr{X}_0$ is the set of initial states, and $t_f \in \mathbb{R}^+$ is the time horizon. The set of input functions is defined as $\mathscr{U}_{[0,t_f]} = \{\mathbf{u}(\cdot) | \mathbf{u}(\cdot) \text{ is piecewise continuous}, \mathbf{u}(t) \in \mathscr{U}, t \in [0,t_f]\}$, where $\mathscr{U}$ is the set of possible input values. The notation $\mathbf{u}(\cdot)$ refers to trajectories rather than the explicit value at time $t$. Note that the commonly used input formulation $\mathbf{B}\,\tilde{\mathbf{u}}(t)$ is included in $\mathbf{u}(t)$ when defining $\mathscr{U} = \{\mathbf{B}\tilde{\mathbf{u}} | \tilde{\mathbf{u}} \in \tilde{\mathscr{U}}\}$.

The objective of this work is to compute the set of reachable states

$$\mathscr{R}^e([0,t_f]) = \Big\{\mathbf{x}\Big|\mathbf{x} = \int_0^t (\mathbf{A}\mathbf{x}(\tau) + \mathbf{u}(\tau))d\tau, \mathbf{A} \in \mathscr{A},$$
$$\mathbf{u}(\cdot) \in \mathscr{U}_{[0,t_f]}, \mathbf{x}(0) \in \mathscr{X}_0, t \in [0,t_f]\Big\}.$$

The fact that $\mathscr{R}^e([0,t_f])$ refers to the exact reachable set is indicated by the superscript $e$. However, the reachable set for uncertain time-invariant linear systems cannot be computed exactly for arbitrary $\mathbf{A}$ and $\mathbf{u}(\cdot)$ [9]. Therefore, overapproximations $\mathscr{R}([0,t_f]) \supseteq \mathscr{R}^e([0,t_f])$ are computed in this work. The task is to find algorithms that bound the overapproximation as tightly as possible, while at the same time ensuring that the algorithms are efficient and scale well with the system dimension $n$. Ensur-

ing tightness of the enclosure is a challenging task due to the wrapping effect, which is understood as the propagation of overapproximations through the computations of successive time steps [29].

The basic principle of many reachability algorithms, including the approach presented here, is to compute the reachable set for consecutive time intervals $\mathscr{R}([t_{k-1}, t_k])$, where $t_k = k \cdot r$ and $k \in \mathbb{N}$ is the time step; see [10, 12, 14, 30]. The complete reachable set is then obtained by: $\mathscr{R}([0, t_f]) = \bigcup_{k=1...t_f/r} \mathscr{R}([t_{k-1}, t_k])$, where $t_f$ is a multiple of $r$. Since the union is represented as a list of the sets $\mathscr{R}([t_{k-1}, t_k])$, the focus of this work is on the computation of a single time interval $[0, r]$. The basic steps for the computation of $\mathscr{R}([0, r])$ are shown in Fig. 2 and are summarized as follows:

1. Computation of the reachable set $\mathscr{H}(r)$ without the input (homogeneous solution), but with consideration of the set $\mathscr{A}$ of system matrices;
2. Generation of the convex hull of the solution at $t = r$ and the initial set;
3. Enlargement of the convex hull to ensure enclosure of all trajectories for the time interval $t \in [0, r]$. The enlargement compensates for two assumptions made in steps 1 and 2: The first assumption was that the system has no input. The second one was that trajectories between the initial set and the reachable set $\mathscr{H}(r)$ are straight lines for which the convex hull computation would be sufficient.
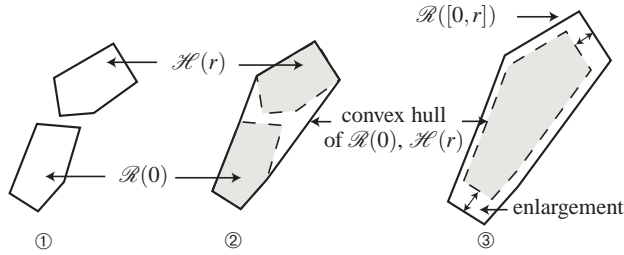


**Fig. 2** Computation of the reachable set for a time interval

It is guaranteed that the formulas derived below return reachable sets that enclose all possible trajectories. The implementation of the algorithms in this work neglects the effect of floating-point errors caused by the finite number of stored digits in computers. This effect can be taken care of by exchanging floating-point arithmetic by interval arithmetic [31], which propagates the rounding errors.

## 3 Overapproximating the Reachable Set

It is well known that the solution of an autonomous linear time-invariant system ($\dot{\mathbf{x}} = \mathbf{A}\mathbf{x}$) is provided by the state transition matrix: $\mathbf{x}(t) = \boldsymbol{\Phi}(t, t_0)\mathbf{x}_0$, where $\boldsymbol{\Phi}(t, t_0) = e^{\mathbf{A}(t-t_0)}$. When the initial state is uncertain within $\mathscr{R}(t_0)$, the set of reachable states

at time $t$ is $\mathscr{R}(t) = \{e^{\mathbf{A}(t-t_0)}\mathbf{x}_0 | \mathbf{x}_0 \in \mathscr{R}(t_0)\}$. If additionally, the system matrix is uncertain, one has to compute the reachable set as $\mathscr{R}(t) = \{e^{\mathbf{A}(t-t_0)}\mathbf{x}_0 | \mathbf{A} \in \mathscr{A}, \mathbf{x}_0 \in \mathscr{R}(t_0)\}$. The computation of the set of possible state transition matrices is discussed first. Then, the extensions for reachable sets of time intervals $[0, r]$ and under the influence of uncertain inputs are presented. Without loss of generality, it is assumed that $t_0 = 0$ from now on, so that $\boldsymbol{\Phi}(t) = \boldsymbol{\Phi}(t, t_0)$.

### 3.1 Overapproximating the State Transition Matrix

In order to make the computation of the set of state transition matrices $\{e^{\mathbf{A}t} | \mathbf{A} \in \mathscr{A}\}$ tractable for matrix zonotopes and interval matrices, some set-based operations have to be computed independently. The set computations that remain dependent are indicated by a special notation. Letting $\circ$ denote either addition or multiplication, then the exact evaluation is denoted by

$$[\![\mathbf{A} \circ \mathbf{A}]\!]_{\mathbf{A} \in \mathscr{A}} := \{\mathbf{A} \circ \mathbf{A} | \mathbf{A} \in \mathscr{A}\}, \tag{1}$$

while an independent evaluation is denoted by

$$\mathscr{A} \circ \mathscr{A} := \{\mathbf{A}_1 \circ \mathbf{A}_2 | \mathbf{A}_1 \in \mathscr{A}, \mathbf{A}_2 \in \mathscr{A}\}.$$

Using an independent evaluation of operands, one obtains an overapproximation in general, e.g.

$$[\![(\mathbf{A} + \mathbf{B})\mathbf{C}]\!]_{\substack{\mathbf{A} \in \mathscr{A} \\ \mathbf{B} \in \mathscr{B} \\ \mathbf{C} \in \mathscr{C}}} \subseteq [\![\mathbf{A}\mathbf{C}]\!]_{\substack{\mathbf{A} \in \mathscr{A} \\ \mathbf{C} \in \mathscr{C}}} + [\![\mathbf{B}\mathbf{C}]\!]_{\substack{\mathbf{B} \in \mathscr{B} \\ \mathbf{C} \in \mathscr{C}}} = \mathscr{A}\mathscr{C} + \mathscr{B}\mathscr{C}.$$

The notation introduced above makes it possible to formulate an overapproximation of the set of matrices $\overline{\mathscr{M}}(t) := [\![e^{\mathbf{A}t}]\!]_{\mathbf{A} \in \mathscr{A}}$ based on the Taylor series of $e^{\mathbf{A}t}$. For typical step sizes in time used in reachability analysis, only the first terms of the Taylor series contribute significantly to the solution. Thus, the dependent set-based evaluation is performed up to second order, while higher order terms are evaluated independently; that is,

$$\begin{aligned}
\overline{\mathscr{M}}(t) &= \left[\!\!\left[ I + \mathbf{A}t + \frac{1}{2!}(\mathbf{A}t)^2 + \frac{1}{3!}(\mathbf{A}t)^3 + \frac{1}{4!}(\mathbf{A}t)^4 + \dots \right]\!\!\right]_{\mathbf{A} \in \mathscr{A}} \\
&\subseteq \left[\!\!\left[ I + \mathbf{A}t + \frac{1}{2!}(\mathbf{A}t)^2 \right]\!\!\right]_{\mathbf{A} \in \mathscr{A}} + \frac{1}{3!}(\mathscr{A}t)^3 + \frac{1}{4!}(\mathscr{A}t)^4 + \dots.
\end{aligned} \tag{2}$$

It is shown below that the computation above is always bounded when the set of matrix values $\mathscr{A}$ and time $t$ is bounded. Thereto, the norm of a set of matrices is defined as

$$\|\mathscr{A}\| = \sup\{\|\mathbf{A}\| \, | \, \mathbf{A} \in \mathscr{A}\}, \tag{3}$$

where $\|\mathbf{A}\|$ denotes an arbitrary matrix norm, while special norms, such as the infinity norm, will be denoted by $\|\mathscr{A}\|_\infty$. Applying the matrix norm, one obtains

$$\|[\![e^{\mathbf{A}t}]\!]_{\mathbf{A}\in\mathscr{A}}\| \leq \sum_{i=0}^{\infty} \frac{1}{i!}\|\mathscr{A}\|^i t^i = e^{\|\mathscr{A}\|t},$$

which is bounded for $\|\mathscr{A}\| < \infty$ and $t < \infty$.

In order to compute $[\![e^{\mathbf{A}t}]\!]_{\mathbf{A}\in\mathscr{A}}$, the infinite sum in (2) has to be replaced by a finite sum to which a set of remainder matrices is added. The number of terms retained in the Taylor series is denoted by $\eta$.

**Proposition 1 (State Transition Matrix Remainder).** *The set of remainder matrices $\sum_{i=\eta+1}^{\infty} \frac{1}{i!}\mathscr{A}^i t^i$ is overapproximated for $|\mathscr{A}| \leq \mathbf{C} \in \mathbb{R}^{n \times n}$ by the interval matrix*

$$\mathscr{E}_{[i]}(t) = [-\mathbf{Y}(t), \mathbf{Y}(t)], \quad \mathbf{Y}(t) = e^{\mathbf{C}t} - \sum_{i=0}^{\eta} \frac{\mathbf{C}^i t^i}{i!}.$$

*The absolute value of a matrix set is defined as the matrix in which each element is equal to the supremum of the absolute value of the corresponding element in each matrix in $\mathscr{A}$. That is, $|\mathscr{A}|_{i,j} = \sup\{|a_{i,j}| \, | \, \mathbf{A} \in \mathscr{A}\}$.*

*Proof.* The multiplication of two matrix sets $\mathscr{A}$ and $\mathscr{B}$, where $C$ and $D$ are chosen such that $|\mathscr{A}| \leq \mathbf{C} \in \mathbb{R}^{n \times n}$ and $|\mathscr{B}| \leq \mathbf{D} \in \mathbb{R}^{n \times n}$, has the absolute value bound $|\mathscr{A}\mathscr{B}| \leq |\mathscr{A}||\mathscr{B}| \leq CD$. From this it follows that $|\mathscr{A}^n| \leq \mathbf{C}^n$ such that

$$\left| \sum_{i=\eta+1}^{\infty} \frac{\mathscr{A}^i t^i}{i!} \right| \leq \sum_{i=\eta+1}^{\infty} \frac{|\mathscr{A}^i| t^i}{i!} \leq \sum_{i=\eta+1}^{\infty} \frac{\mathbf{C}^i t^i}{i!} = e^{\mathbf{C}t} - \sum_{i=0}^{\eta} \frac{\mathbf{C}^i t^i}{i!}. \qquad \square$$

Besides the presented Taylor method, there is a number of different techniques to compute the matrix exponential [32]. Unfortunately, these alternative approaches are not suitable for computations with matrix sets or do not provide error bounds. No error bounds can be provided when applying techniques which use solvers of ordinary differential equations [32]. Polynomial methods make it possible to obtain the matrix exponential from a finite sum $e^{At} = \sum_{i=0}^{n-1} \alpha_i(t) A^i$, where $\alpha_i(t)$ is a polynomial. However, the error introduced by the Taylor series remainder, which would be omitted using this technique, is small compared to the computation of the powers $\mathscr{A}^i$. Matrix decomposition methods, where $A = SBS^{-1}$ so that $e^{At} = Se^{Bt}S^{-1}$ suffer from the problem that the inverse of an uncertain matrix is hard to compute [33] and that for many techniques $S$ is hard to obtain when $A$ is uncertain, e.g. when $S$ is a matrix of eigenvectors [34]. Splitting techniques which are based on the formula $e^{B+C} = \lim_{m \to \infty} (e^{B/m}e^{C/m})^m$ are not appropriate, too, since high powers of matrix sets are hard to compute.

## 3.2 Reachable Sets of Time Intervals

Given the homogeneous solution $\mathbf{x}_h(r) \in \overline{\mathscr{M}}(r)\mathbf{x}(0)$, the following approximation for the solution at intermediate points in time is suggested:

$$\hat{\mathbf{x}}_h(t) = \mathbf{x}(0) + \frac{t}{r}(\mathbf{M}\mathbf{x}(0) - \mathbf{x}(0)), \quad \mathbf{M} \in \overline{\mathscr{M}}(r), t \in [0, r]. \tag{4}$$

The error $\mathbf{x}_h(t) - \hat{\mathbf{x}}_h(t)$ made when applying this approximation is bounded by the set $\mathscr{F}(r)\mathbf{x}(0)$, where $\mathscr{F}(r)$ is a set of matrices such that $\mathbf{x}_h(t) \in \hat{\mathbf{x}}_h(t) + \mathscr{F}(r)\mathbf{x}(0)$. Using the inclusion $\mathbf{x}_h(t) \in \overline{\mathscr{M}}(t)\mathbf{x}(0)$ and replacing $\overline{\mathscr{M}}(t)$ by its Taylor series yields a formula for computing the set of matrices $\mathscr{F}$:

$$\mathscr{F}(r) \supseteq \left\{ \sum_{i=0}^{\eta} \frac{\mathbf{A}_i t^i}{i!} + \mathscr{E}_{[i]}(t) - \mathbf{I} - \frac{t}{r}\left(\sum_{i=0}^{\infty} \frac{\mathbf{A}_i r^i}{i!} + \mathscr{E}_{[i]}(r) - \mathbf{I}\right) \middle| \mathbf{A}_i \in \mathscr{A}^i, t \in [0, r] \right\}$$

$$= \left\{ \sum_{i=2}^{\eta} \frac{\mathscr{A}^i}{i!}(t^i - tr^{i-1}) + \mathscr{E}_{[i]}(t) - \frac{t}{r}\mathscr{E}_{[i]}(r) \middle| t \in [0, r] \right\}.$$

In [27] it is shown that

$$[\varphi](i, r) := \left\{ t^i - tr^{i-1} \middle| t \in [0, r] \right\} = \left[ (i^{\frac{-i}{i-1}} - i^{\frac{-1}{i-1}})r^i, 0 \right].$$

It remains to compute $\mathscr{E}_{[i]}(t) - \frac{t}{r}\mathscr{E}_{[i]}(r)$. The matrix set $\mathscr{E}_{[i]}(t)$ is strictly increasing with time so that $\mathscr{E}_{[i]}(t) \in [0, 1]\mathscr{E}_{[i]}(r)$ for $t \in [0, r]$. Thus,

$$\left\{ \mathscr{E}_{[i]}(t) - \frac{t}{r}\mathscr{E}_{[i]}(r) \middle| t \in [0, r] \right\} \subseteq \left\{ (\mu_1 - \mu_2)\mathscr{E}_{[i]}(r) \middle| \mu_1, \mu_2 \in [0, 1] \right\} = [-1, 1]\mathscr{E}_{[i]}(r)$$

and $[-1, 1]\mathscr{E}_{[i]}(r) = \mathscr{E}_{[i]}(r)$ because $\mathscr{E}_{[i]}(t)$ has symmetric bounds. These simplifications make it possible to compute $\mathscr{F}(r)$ as

$$\mathscr{F}(r) = \sum_{i=2}^{\eta} \frac{\mathscr{A}^i}{i!}[\varphi](i, r) + \mathscr{E}_{[i]}(r).$$

Since all possible solutions of (4) are contained in the convex hull $\mathtt{CH}(R(0) \cup \overline{\mathscr{M}}(r)\mathscr{R}(0))$, the reachable set for a time interval without input can be computed as $\mathscr{R}([0, r]) = \mathtt{CH}(\mathscr{R}(0) \cup \overline{\mathscr{M}}(r)\mathscr{R}(0)) + \mathscr{F}(r)\mathscr{R}(0)$.

## 3.3 Reachable Set of the Complete System

We now consider the additional contribution to the reachable set due to uncertain inputs. Since the superposition principle for linear systems can be applied, the reachable set of the input solution can be computed independently of the homogeneous solution. The input solution $\mathbf{x}_p(t)$ is bounded according to [35, Chap. 3] by

$$\mathbf{x}_p(t) \in \int_{t_0}^{t} \overline{\mathscr{M}}(t-\tau)\mathbf{u}(\tau)d\tau, \quad t \geq t_0. \tag{5}$$

In order to compute the reachable set due to uncertain inputs, the following proposition on distributivity of positive scalars and convex matrix sets is required.

**Proposition 2 (Distributivity of Matrix Sets).** *When $\mathscr{A}$ is convex and $a,b \in \mathbb{R}^+$:*

$$a\mathscr{A} + b\mathscr{A} = (a+b)\mathscr{A}.$$

*Proof.* It is always true that $(a+b)\mathscr{A} \subseteq a\mathscr{A} + b\mathscr{A}$, even if $\mathscr{A}$ is not convex. Further, due to the convexity it follows for the real-valued and arbitrary matrices $\mathbf{X}_1, \mathbf{X}_2 \in \mathscr{A}$ and the scalar $\alpha \in [0,1]$ that $\alpha\mathbf{X}_1 + (1-\alpha)\mathbf{X}_2 \in \mathscr{A}$. Making use of $a,b \geq 0$ this can be rewritten by choosing $\alpha = \frac{a}{a+b}$:

$$\frac{a}{a+b}\mathbf{X}_1 + \frac{b}{a+b}\mathbf{X}_2 \in \mathscr{A}$$

so that $a\mathbf{X}_1 + b\mathbf{X}_2 \in (a+b)\mathscr{A}$ and consequently $a\mathscr{A} + b\mathscr{A} \subseteq (a+b)\mathscr{A}$.    □

**Theorem 1 (Input Solution).** *The set of reachable states due to the uncertain input* $\mathbf{u}(t) \in \mathscr{U}$ *is overapproximated as*

$$\mathscr{P}(t) = \sum_{i=0}^{\eta} \left( \frac{\mathrm{CH}(\mathscr{A}^i\mathscr{U})t^{i+1}}{(i+1)!} \right) + \mathscr{E}_{[i]}(t)\,t\,|\mathscr{U}|.$$

*Proof.* The integral in (5) is solved for set-valued inputs by splitting the integral from $t_0$ to $t$ into subintervals $[t_k, t_{k+1}]$, where $k \in \{0, \ldots, m-1\}$. For now, it is assumed that the input value taken from $\mathscr{U}$ is constant within time intervals $[t_k, t_{k+1}]$, so that $\mathscr{U}$ can be excluded from the integration:

$$\mathbf{x}_p(t) \in \sum_{k=0}^{m-1} \int_{t_k}^{t_{k+1}} \overline{\mathscr{M}}(t-\tau)d\tau\,\mathscr{U}. \tag{6}$$

This assumption will be overruled when choosing $m \to \infty$ later. Next, $\overline{\mathscr{M}}(t-\tau) = \sum_{i=0}^{\eta} \mathscr{A}^i(t-\tau)^i/i! + \mathscr{E}_{[i]}(t-\tau)$ is inserted so that

$$\int_{t_k}^{t_{k+1}} \overline{\mathscr{M}}(t-\tau)d\tau = \sum_{i=0}^{\eta} \frac{\mathscr{A}^i}{i!} \underbrace{\int_{t_k}^{t_{k+1}} (t-\tau)^i d\tau}_{=\int_{t-t_{k+1}}^{t-t_k} \tau^i d\tau} + \underbrace{\int_{t_k}^{t_{k+1}} \mathscr{E}_{[i]}(t-\tau)d\tau}_{=\int_{t-t_{k+1}}^{t-t_k} \mathscr{E}_{[i]}(\tau)d\tau} \tag{7}$$

The integral in (7) can be moved inside since the matrix values within $\mathscr{A}$ are not time-varying. Inserting (7) into (6) yields

$$\mathbf{x}_p(t) \in \sum_{k=0}^{m-1} \left( \sum_{i=0}^{\eta} \frac{\mathscr{A}^i}{i!} \int_{t-t_{k+1}}^{t-t_k} \tau^i d\tau + \int_{t-t_{k+1}}^{t-t_k} \mathscr{E}_{[i]}(\tau)d\tau \right) \mathscr{U}$$

Using $\sum_{k=0}^{m-1} \int_{t-t_{k+1}}^{t-t_k} \mathscr{E}_{[i]}(\tau)d\tau|\mathscr{U}| = \int_0^t \mathscr{E}_{[i]}(\tau)d\tau|\mathscr{U}|$, where $|\mathscr{U}|$ returns an axis-aligned box, and applying Prop. 2 yields

$$\mathbf{x}_p(t) \in \sum_{i=0}^{\eta} \frac{\text{CH}(\mathscr{A}^i\mathscr{U})}{i!} \underbrace{\int_0^t \tau^i d\tau}_{=t^{i+1}/(i+1)} + \int_0^t \mathscr{E}_{[i]}(\tau)d\tau|\mathscr{U}|.$$

One can see that the result is independent of the number $m$ of intermediate time intervals due to Prop. 2. This means that choosing $m \to \infty$ returns the same result so that the assumption of constant input values within time intervals can be overruled. It remains to compute the integral $[-\tilde{\mathbf{Y}}(t), \tilde{\mathbf{Y}}(t)] := \int_0^t \mathscr{E}_{[i]}(\tau)d\tau$, where

$$\tilde{\mathbf{Y}}(t) = \sum_{i=\eta+1}^{\infty} \frac{\mathbf{C}^i}{(i+1)!}t^{i+1} < \sum_{i=\eta+1}^{\infty} \frac{\mathbf{C}^i}{i!}t^{i+1} = \mathbf{Y}(t)t,$$

so that $\int_0^t \mathscr{E}_{[i]}(\tau)d\tau \subset \mathscr{E}_{[i]}(t)t$ and $\mathbf{Y}(t)$ is as introduced in Prop. 1. $\qquad\square$

If the origin is contained in the set of possible inputs ($0 \in \mathscr{U}$), it holds that $\mathscr{P}([0,r]) = \mathscr{P}(r)$; see [27]. If this is not the case, some minor extensions are required [27]. Assuming that $0 \in \mathscr{U}$, the overall algorithm for computing the reachable set can be stated in Algorithm 1.

---

**Algorithm 1** Compute $\mathscr{R}([0,t_f])$

---

**Input:** Initial set $\mathscr{R}(0)$, set of state transition matrices $\overline{\mathscr{M}}(r)$, input set $\mathscr{U}$, set of correction matrices $\mathscr{F}(r)$, time increment $r$, time horizon $t_f$
**Output:** $\mathscr{R}([0,t_f])$

$\mathscr{H}_0 = \text{CH}(\mathscr{R}(0) \cup \overline{\mathscr{M}}(r)\mathscr{R}(0)) + \mathscr{F}(r)\mathscr{R}(0)$
$\mathscr{P}_0 = \sum_{i=0}^{\eta} \left( \frac{\text{CH}(\mathscr{A}^i\mathscr{U})r^{i+1}}{(i+1)!} \right) + \mathscr{E}_{[i]}(r)r|\mathscr{U}|$
$\mathscr{R}_0 = \mathscr{H}_0 + \mathscr{P}_0$
**for** $k = 1 \ldots \frac{t_f}{r} - 1$ **do**
$\quad \mathscr{R}_k = \overline{\mathscr{M}}(r)\mathscr{R}_{k-1} + \mathscr{P}_0$
**end for**
$\mathscr{R}([0,t_f]) = \bigcup_{k=1}^{t_f/r} \mathscr{R}_{k-1}$

---

## 4 Overapproximating the State Transition Matrix

The computation of the set of possible state transition matrices $\{e^{\mathbf{A}t}|\mathbf{A} \in \mathscr{A}\}$ using matrix zonotopes and interval matrices as representation of the matrix set $\mathscr{A}$ are discussed next. Matrix zonotopes are more general than interval matrices, while the presented computations are more efficient using interval matrices. The presented

techniques still work when the set of matrices $\mathscr{A}$ contains matrices for which the linear system is unstable. This is useful when considering hybrid systems with switched linear dynamics, where some linear systems are unstable, while the overall dynamics is stable.

## 4.1 Matrix Zonotopes

A matrix zonotope is defined as

$$\mathscr{A}_{[z]} = \left\{ \mathbf{G}^{(0)} + \sum_{i=1}^{\kappa} p_i \mathbf{G}^{(i)} \Big| p_i \in [-1,1], \mathbf{G}^{(i)} \in \mathbb{R}^{n \times n} \right\} \tag{8}$$

and is written in short form as $\mathscr{A}_{[z]} = (\mathbf{G}^{(0)}, \mathbf{G}^{(1)}, \ldots, \mathbf{G}^{(\kappa)})$, where the first matrix is referred to as the *matrix center* and the other matrices as *matrix generators*. The order of a matrix zonotope is defined as $\rho = \kappa/n$. When exchanging the matrix generators by vector generators $g^{(i)} \in \mathbb{R}^n$, one obtains a zonotope (see e.g. [14]). Matrix zonotopes can also be represented as the convex hull of its so-called matrix vertices $\mathbf{V}^{(i)}$:

$$\mathscr{A}_{[z]} = \left\{ \sum_{i=1}^{r} \alpha_i \mathbf{V}^{(i)} \Big| \mathbf{V}^{(i)} \in \mathbb{R}^{n \times n}, \alpha_i \in \mathbb{R}, \alpha_i \geq 0, \sum_i \alpha_i = 1 \right\}. \tag{9}$$

In order to obtain the Taylor series terms in (2), one has to compute the power of matrix zonotopes. This is done iteratively by $\mathscr{A}_{[z]}^l = \mathscr{A}_{[z]} \mathscr{B}_{[z]}$, where $\mathscr{B}_{[z]} = \mathscr{A}_{[z]}^{l-1}$. Thus, it suffices to show the multiplication of two matrix zonotopes $\mathscr{A}_{[z]} = (\mathbf{G}^{(0)}, \ldots, \mathbf{G}^{(\kappa_A)})$ and $\mathscr{B}_{[z]} = (\mathbf{H}^{(0)}, \ldots, \mathbf{H}^{(\kappa_B)})$:

$$
\begin{aligned}
\mathscr{A}_{[z]} \mathscr{B}_{[z]} &= \left[\!\!\left[ \left( \mathbf{G}^{(0)} + \sum_{i=1}^{\kappa_A} p_i \mathbf{G}^{(i)} \right) \left( \mathbf{H}^{(0)} + \sum_{j=1}^{\kappa_B} q_j \mathbf{H}^{(j)} \right) \right]\!\!\right]_{p_i, q_j \in [-1,1]} \\
&= \mathbf{G}^{(0)} \mathbf{H}^{(0)} + \sum_{\substack{i=0 \\ (i,j) \neq (0,0)}}^{\kappa_A} \sum_{j=0}^{\kappa_B} \underbrace{[\![ p_i q_j ]\!]_{p_i, q_j \in [-1,1]}}_{\subseteq [-1,1]} \mathbf{G}^{(i)} \mathbf{H}^{(j)},
\end{aligned}
\tag{10}
$$

so that $\mathscr{A}_{[z]} \mathscr{B}_{[z]} \subseteq (\mathbf{G}^{(0)} \mathbf{H}^{(0)}, \mathbf{G}^{(0)} \mathbf{H}^{(1)}, \ldots, \mathbf{G}^{(\kappa_A)} \mathbf{H}^{(\kappa_B)})$. The Taylor terms up to second order are evaluated exactly:

**Proposition 3 (Dependent Matrix Zonotope Evaluation).** *The set* $[\![ \mathbf{I} + \mathbf{A}t + 1/2(\mathbf{A}t)^2 ]\!]_{\mathbf{A} \in \mathscr{A}_{[z]}}$, *where* $\mathscr{A}_{[z]} = (\mathbf{G}^{(0)}, \mathbf{G}^{(1)}, \ldots, \mathbf{G}^{(\kappa_A)})$ *is enclosed by the smallest possible zonotope* $\mathscr{W}_{[z]}(t) = (\mathbf{L}^{(0)}(t), \mathbf{L}^{(1)}(t), \ldots, \mathbf{L}^{(\kappa_W)}(t))$, *where*

$$
\begin{aligned}
& \mathbf{L}^{(0)}(t) && = \mathbf{I} + \mathbf{G}^{(0)}t + \left(\mathbf{G}^{(0)^2} + \sum_{i=1}^{\kappa_A} 0.5\mathbf{G}^{(i)^2}\right)t^2, \\
j = 1\ldots\kappa_A: \quad & \mathbf{L}^{(j)}(t) && = \mathbf{G}^{(j)}t + (\mathbf{G}^{(0)}\mathbf{G}^{(j)} + \mathbf{G}^{(j)}\mathbf{G}^{(0)})t^2, \\
j = 1\ldots\kappa_A: \quad & \mathbf{L}^{(\kappa_A+j)}(t) && = 0.5\mathbf{G}^{(j)^2}t^2, \\
l = \sum_{j=1}^{\kappa_A-1}\sum_{k=j+1}^{\kappa_A} 1: \quad & \mathbf{L}^{(2\kappa_A+l)}(t) && = (\mathbf{G}^{(j)}\mathbf{G}^{(k)} + \mathbf{G}^{(k)}\mathbf{G}^{(j)})t^2.
\end{aligned}
$$

*Proof.* The result of the multiplication $(\mathbf{G}^{(0)} + \sum_{i=1}^{\kappa_A} p_i\mathbf{G}^{(i)})(\mathbf{G}^{(0)} + \sum_{i=1}^{\kappa_A} p_i\mathbf{G}^{(i)})$ can be rearranged to

$$
\mathbf{G}^{(0)^2} + \sum_{j=1}^{\kappa_A} p_j(\mathbf{G}^{(0)}\mathbf{G}^{(j)} + \mathbf{G}^{(j)}\mathbf{G}^{(0)}) + \sum_{j=1}^{\kappa_A} p_j^2\mathbf{G}^{(j)^2}
$$
$$
+ \sum_{j=1}^{\kappa_A-1}\sum_{k=j+1}^{\kappa_A} p_j p_k(\mathbf{G}^{(j)}\mathbf{G}^{(k)} + \mathbf{G}^{(k)}\mathbf{G}^{(j)}),
$$

where $p_j, p_k \in [-1,1]$ and $p_j^2 \in [0,1]$. Since the interval $[0,1]$ deviates from $[-1,1]$ used as factors for matrix generators, it is split into $0.5 + [-1,1]0.5$; this makes it possible to add the matrices $0.5\mathbf{G}^{(j)^2}$ to the constant solution $\mathbf{G}^{(0)^2}$, and use the same matrix values as generator matrices. Applying this result to $[\![\mathbf{I} + \mathbf{A}t + 1/2(\mathbf{A}t)^2]\!]_{\mathbf{A}\in\mathscr{A}_{[z]}}$ results in the above proposition. $\qquad\square$

## 4.2 Interval Matrices

An interval matrix is a special case of a matrix zonotope and specifies for each matrix element the interval of possible values:

$$
\mathscr{A}_{[i]} = [\underline{\mathbf{A}}, \overline{\mathbf{A}}], \quad \forall i,j: \underline{a}_{ij} \leq \overline{a}_{ij}, \quad \underline{\mathbf{A}}, \overline{\mathbf{A}} \in \mathbb{R}^{n\times n}.
$$

The matrix $\underline{\mathbf{A}}$ is referred to as the *lower bound* and $\overline{\mathbf{A}}$ as the *upper bound* of $\mathscr{A}_{[i]}$.

When computing with intervals, one generally uses interval arithmetic. In this work, only the addition and multiplication rule are required:

$$
\begin{aligned}
[a] + [b] &= [\underline{a} + \underline{b}, \overline{a} + \overline{b}], \\
[a] \cdot [b] &= [\min(\underline{a}\underline{b}, \underline{a}\overline{b}, \overline{a}\underline{b}, \overline{a}\overline{b}), \max(\underline{a}\underline{b}, \underline{a}\overline{b}, \overline{a}\underline{b}, \overline{a}\overline{b})].
\end{aligned} \tag{11}
$$

For the computation of the Taylor terms $\frac{1}{l!}(\mathscr{A}_{[i]}t)^i$, one has to compute the power of interval matrices. This is done iteratively as for matrix zonotopes by $\mathscr{A}_{[i]}^l = \mathscr{A}_{[i]}\mathscr{B}_{[i]}$, where $\mathscr{B}_{[i]} = \mathscr{A}_{[i]}^{l-1}$. Using interval arithmetic, $\mathscr{C}_{[i]} = \mathscr{A}_{[i]}\mathscr{B}_{[i]}$ is computed element-wise by the single-use expression $[c_{ij}] = \sum_{k=1}^{n}[a_{ik}][b_{kj}]$, i.e. each matrix value occurs only once for each computation of $[c_{ij}]$. In interval arithmetic, single use expressions are always exact, e.g. $[a]([b]+1) = [\![a(b+1)]\!]_{a\in[a],b\in[b]}$. However, in this case, $\mathscr{B}_{[i]}$ is a function of $\mathscr{A}_{[i]}$ such that $\mathscr{C}_{[i]} \supseteq \mathscr{A}_{[i]}\mathscr{B}_{[i]}$.

In [36] it has been shown that the square of an interval matrix can be rewritten as a single-use expression, making the computation exact using interval arithmetic, i.e. the tightest possible interval matrix is computed. It has been further proven in [36] that it is NP-hard to compute the tightest enclosing interval matrix of the cube of an interval matrix ($\mathscr{A}_{[i]}{}^3$). The idea of computing the square of an interval matrix is extended in order to write as many computations of $[\![\mathbf{I}+\mathbf{A}t+1/2(\mathbf{A}t)^2]\!]_{\mathbf{A}\in\mathscr{A}_{[i]}}$ as a single-use expression, while the other expressions are evaluated by computing the global maxima.

**Proposition 4 (Dependent Interval Matrix Evaluation).** *The set* $[\![\mathbf{I}+\mathbf{A}t+1/2(\mathbf{A}t)^2]\!]_{\mathbf{A}\in\mathscr{A}_{[i]}}$ *can be tightly enclosed by another interval matrix* $\mathscr{W}_{[i]}(t) = [\underline{\mathbf{W}}(t),\overline{\mathbf{W}}(t)]$, *where*

$$\forall i \neq j : [w_{ij}] = [a_{ij}]\left(t + \frac{1}{2}([a_{ii}]+[a_{jj}])t^2\right) + \frac{1}{2}\sum_{k:k\neq i,k\neq j}[a_{ik}][a_{kj}]t^2$$

$$\forall i : [w_{ii}] = \left[\kappa([a_{ii}],t), \max\left(\underline{a}_{ii}t + \frac{1}{2}\underline{a}_{ii}^2t^2, \overline{a}_{ii}t + \frac{1}{2}\overline{a}_{ii}^2t^2\right)\right] + \frac{1}{2}\sum_{k:k\neq i}[a_{ik}][a_{ki}]t^2$$

$$\kappa([a_{ii}],t) = \begin{cases} \min\left(\{\underline{a}_{ii}t + \frac{1}{2}\underline{a}_{ii}^2t^2, \overline{a}_{ii}t + \frac{1}{2}\overline{a}_{ii}^2t^2\}\right), & \text{for} -\frac{1}{t} \notin [a_{ii}] \\ -\frac{1}{2}, & \text{for} -\frac{1}{t} \in [a_{ii}] \end{cases}$$

*Proof.* The non-diagonal elements $[w_{ij}]$ can be formulated as a single-use expression (SUE), resulting in an exact evaluation using interval arithmetic. The computation of the diagonal elements $[w_{ii}]$ cannot entirely be reformulated to a SUE. However, one can split $[w_{ii}]$ into a part with and without a single variable occurrence:

$$[w_{ii}] = \underbrace{[a_{ii}]t + \frac{1}{2}[a_{ii}]^2t^2}_{\text{non-SUE}} + \underbrace{\frac{1}{2}\sum_{k:k\neq i}[a_{ik}][a_{ki}]t^2}_{\text{SUE}}.$$

It remains to obtain the exact interval of $\gamma(a) := at + \frac{1}{2}a^2t^2$ by computing the minimum and maximum. The function $\gamma(a)$ has only one minimum at $a = -1/t$ and is monotone elsewhere, so that the maximum is to be found at the borders: $\gamma_{max} = \max(\underline{a}_{ii}t + \frac{1}{2}\underline{a}_{ii}^2t^2, \overline{a}_{ii}t + \frac{1}{2}\overline{a}_{ii}^2t^2)$. Where the global minimum ($a_{min} = -1/t$) is an element of $[a_{ii}]$, one obtains: $\gamma_{min} = -1/2$. In the other case, the minimum is to be found at the border: $\gamma_{min} = \min(\underline{a}_{ii}t + \frac{1}{2}\underline{a}_{ii}^2t^2, \overline{a}_{ii}t + \frac{1}{2}\overline{a}_{ii}^2t^2)$.                     □

Besides computing with the lower and upper bound of intervals, one can also compute with the center and the radius of the interval. The advantage of the latter technique is that it is more efficient and easier to parallelize; see [31]. The result is more conservative, but the interval of a standard operation (addition, difference, multiplication, and division) is bounded by a factor 1.5 in radius[1] compared to the computation with lower and upper bounds.

---

[1] The radius of a set $X$ is defined as $0.5\max_{x_1\in X, x_2\in X}|x_1-x_2|$ in [31].

### 4.3 Norm Bounds

In order to quickly estimate the size of the set of state transition matrices, it is often helpful to compute with norms instead of applying the introduced computational techniques using matrix zonotopes or interval matrices.

**Theorem 2 (Norm Bound).** *In order to obtain a tight norm bound, the matrix set $\mathscr{A}$ is overapproximated by an interval matrix $\mathscr{A}_{[i]}$ which is split into a nominal and a symmetric part: $\mathscr{A}_{[i]} = \mathbf{A}_{[n]} + [-\mathbf{S}, \mathbf{S}]$. The norm of the distance of the set of state transition matrices to the exponential matrix of the nominal matrix is computed for $\|\|\mathbf{A}_{[n]}\| + \mathbf{S}\| < \frac{2}{t}$ as*

$$\|[\![e^{\mathbf{A}t}]\!]_{\mathbf{A} \in \mathscr{A}} - e^{\mathbf{A}_{[n]}t}\|$$

$$\leq \frac{\|\mathbf{A}_{[n]}\| \, \|\mathbf{S}\| \frac{t^2}{2}}{\|\mathbf{A}_{[n]}\| \cdot \|\|\mathbf{A}_{[n]}\| + \mathbf{S}\| \frac{t^2}{4} - (\|\mathbf{A}_{[n]}\| + \|\|\mathbf{A}_{[n]}\| + \mathbf{S}\|) \frac{t}{2} + 1} + \frac{\|\mathbf{S}\|t}{1 - \|\|\mathbf{A}_{[n]}\| + \mathbf{S}\| \frac{t}{2}}.$$

The proof is shown in the Appendix.

### 4.4 Discussion

For small times $t < 2/(\|\|\mathbf{A}_{[n]}\| + \mathbf{S}\|)$ (see the Appendix), which are typically used for reachability analysis, the terms $\frac{1}{i!}(\mathscr{A}t)^i$ contribute less to the overall solution $[\![e^{\mathbf{A}t}]\!]_{\mathbf{A} \in \mathscr{A}}$ for increasing $i$ values. Thus, one should use sophisticated computations for the first terms and switch to coarser and more efficient computations for higher order terms. For this reason, computations with matrix zonotopes are only conducted up to second order in this work. Another reason is that the number of generators for the $l^{th}$ power is $(\kappa + 1)^l - 1$, while the representation size does not grow for interval matrices. In order to keep the overapproximation of interval computations low, higher powers are based on the exact result of the square; see [36]. Besides matrix zonotopes, one can also represent uncertainties by the more general matrix polytopes [27]. However, due to the computational complexity of matrix polytopes, it is advisable to overapproximate them by matrix zonotopes (see [27]) and compute with the methods presented herein.

### 4.5 Numerical Evaluation of the Set of State Transition Matrices

The methods presented for computing the set of state transition matrices are illustrated for a five-dimensional example and evaluated for randomly generated examples.

### 4.5.1 Five-Dimensional Example

The computation of the set of state transition matrices is demonstrated for the matrix zonotope

$$
\mathscr{A}_{[z]} = (\mathbf{G}^{(0)}, \mathbf{G}^{(1)}), \quad \mathbf{G}^{(0)} = \begin{bmatrix} -1 & -4 & 0 & 0 & 0 \\ 4 & -1 & 0 & 0 & 0 \\ 0 & 0 & -3 & 1 & 0 \\ 0 & 0 & -1 & -3 & 0 \\ 0 & 0 & 0 & 0 & -2 \end{bmatrix}, \mathbf{G}^{(1)} = \begin{bmatrix} 0.1 & 0.1 & 0 & 0 & 0 \\ 0.1 & 0.1 & 0 & 0 & 0 \\ 0 & 0 & 0.1 & 0.1 & 0 \\ 0 & 0 & 0.1 & 0.1 & 0 \\ 0 & 0 & 0 & 0 & 0.1 \end{bmatrix}.
$$

(12)

and the corresponding interval matrix that tightly encloses the above matrix zonotope:

$$
\mathscr{A}_{[i]} = \begin{bmatrix} [-1.1, -0.9] & [-4.1, -3.9] & 0 & 0 & 0 \\ [3.9, 4.1] & [-1.1, -0.9] & 0 & 0 & 0 \\ 0 & 0 & [-3.1, -2.9] & [0.9, 1.1] & 0 \\ 0 & 0 & [-1.1, -0.9] & [-3.1, -2.9] & 0 \\ 0 & 0 & 0 & 0 & [-2.1, -1.9] \end{bmatrix}.
$$

(13)

The resulting sets $\overline{\mathscr{M}}(t)$ are computed for $t = 0.05$ and the maximum order $\eta = 6$ of the Taylor expansion. For the matrix zonotope $\mathscr{A}_{[z]}$, the set of state transition matrices is plotted for selected projections in Fig. 3. Particular matrix exponential values generated from matrix samples $\check{\mathbf{A}}_i \in \mathscr{A}_{[z]}$ are also plotted. These matrices are the vertex matrices of $\mathscr{A}_{[z]}$ and 100 randomly chosen matrices. One can observe that the matrix zonotope computation is much more accurate and captures very well the result of the samples, while the interval matrix computation returns a much larger set. The independent evaluation of each Taylor term using matrix zonotopes, i.e. (10) is applied for the first two Taylor terms instead of Prop. 3, also returns a much larger compared to the dependent evaluation of the terms up to second order.

The results for the interval matrix $\mathscr{A}_{[i]}$ are shown in Fig. 4. Obviously, the computation with matrix zonotopes results only in marginal improvements when the uncertain matrix is an interval matrix, while it is a more significant improvement over the independent evaluation, i.e. pure interval arithmetic is applied for the first two Taylor terms instead of Prop. 4. For interval matrices, the result is tight for both, the interval matrix and the matrix zonotope computation.

### 4.5.2 Random Matrix Set Generation

For a more thorough evaluation, random matrix sets are computed using a number of characterizing parameters. A random matrix whose elements are uniformly distributed is denoted by $\mathbf{A}^{\text{rand}} = \text{rand}(\overline{a}, \mu)$ so that $\forall i, j : -\overline{a} \leq a_{ij}^{\text{rand}} \leq \overline{a}$. The variable $\mu$ determines the ratio of the number of non-zero elements to all elements of a

(a) Projection onto $\overline{\mathscr{M}}_{12}, \overline{\mathscr{M}}_{22}$.          (b) Projection onto $\overline{\mathscr{M}}_{43}, \overline{\mathscr{M}}_{34}$.
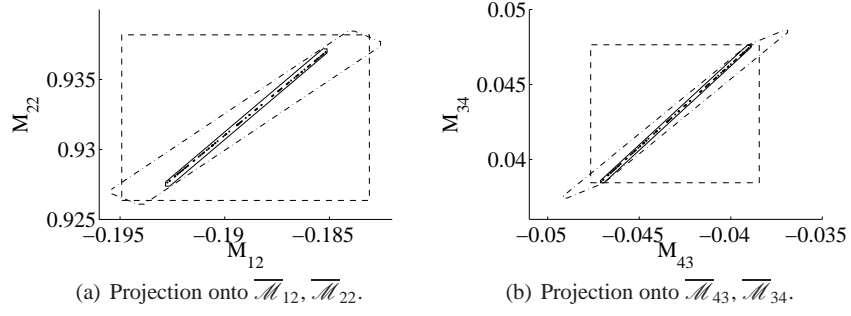
**Fig. 3** Computations of $\overline{\mathscr{M}}(t)$ for the set $\mathscr{A}_{[z]}$ as specified in (12); $t = 0.05, \eta = 6$. Solid line: matrix zonotope computation; dashed line: interval matrix computation; dash-dotted line: independent matrix zonotope computation, i.e. independent evaluation of each Taylor term
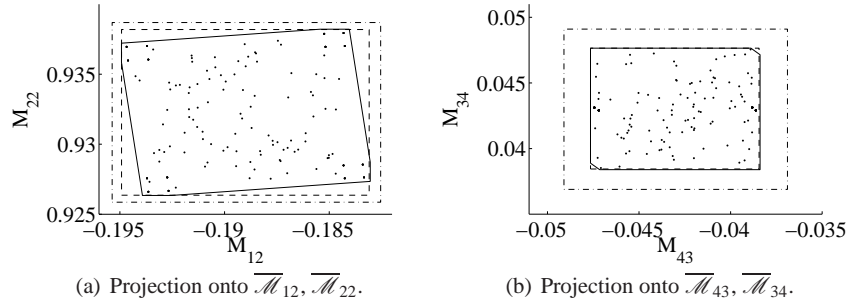


(a) Projection onto $\overline{\mathscr{M}}_{12}, \overline{\mathscr{M}}_{22}$.          (b) Projection onto $\overline{\mathscr{M}}_{43}, \overline{\mathscr{M}}_{34}$.

**Fig. 4** Computations of $\overline{\mathscr{M}}(t)$ for the set $\mathscr{A}_{[i]}$ as specified in (13); $t = 0.05, \eta = 6$. Solid line: matrix zonotope computation; dashed line: interval matrix computation; dash-dotted line: independent matrix zonotope computation, i.e. independent evaluation of each Taylor term

matrix, i.e. the number of non-zero values is `ceil`$(\mu n^2)$ and `ceil` returns the next higher natural number.

The matrix center and matrix generators are randomly generated as $\mathbf{G}^{(0)} = $ `rand`$(\sigma, 1)$ and $\mathbf{G}^{(i)} = $ `rand`$(\frac{1}{\kappa}, \mu)$, where $\sigma$ is referred to as center-uncertainty ratio, $\kappa$ is the number of generators, and $\mu$ is the non-zero ratio. Note that the non-zero elements have the same row and column indices for all generator matrices so that the corresponding interval matrix uncertainties are non-zero at the same positions. The interval enclosure of matrix zonotopes is equivalent to generating interval matrices $\mathbf{G}^{(0)} + [-\mathbf{S}, \mathbf{S}]$, where $\mathbf{S} = $ `rand`$(1, \mu)$.

There are no further constraints on the generation of random matrix sets, such that the sets might contain stable and/or unstable matrices.

### 4.5.3 Norm Evaluation

As a first test, the norm $\|\mathscr{M}(t) - \mathbf{M}_{[n]}(t)\|_\infty$ with $\mathbf{M}_{[n]}(t) = e^{\mathbf{A}_{[n]}t}$ as defined in (3) is over- and underapproximated. The underapproximation is obtained as a union of sampled matrices: $\underline{\mathscr{M}}(t) = \bigcup_{i=1}^{\varpi} e^{\check{\mathbf{A}}^{(i)}t}$, where $\check{\mathbf{A}}^{(i)}$ are vertex matrices and $10^3$ randomly generated matrices.

The overapproximation is obtained as presented above and the inf-norm when computing with interval matrices can easily be computed as $\|\mathscr{A}_{[i]}\|_\infty = \|A^*\|_\infty$, where $a_{ij}^* = \max(|\underline{a}_{ij}|, |\overline{a}_{ij}|)$. Note that computing the 2-norm of an interval matrix is exponential in the system dimension [37]. When the set of uncertain matrices is from the class of matrix zonotopes, the maximum norm is to be found equal to one of the vertex matrices $\mathbf{V}^{(i)}$ since $\|\sum_{i=1}^{r_A} \alpha_i \mathbf{V}^{(i)}\| \le \sum_{i=1}^{r_A} \alpha_i \|\mathbf{V}^{(i)}\|$, $\alpha_i \ge 0$ (see (9)). However, the number of vertices is too high, even in small dimensions, such that only interval matrices can be evaluated. This is obvious since already the number of vertex matrices required to represent the remainder $\mathscr{E}_{[i]}$ is $2^{n^2}$ when each element of $\mathscr{E}_{[i]}$ is uncertain within an interval.

The ratio of both norms is defined as

$$\theta = \frac{\|\overline{\mathscr{M}}(t) - \mathbf{M}_{[n]}(t)\|_\infty}{\|\underline{\mathscr{M}}(t) - \mathbf{M}_{[n]}(t)\|_\infty}$$

and its evaluation is performed using randomly generated interval matrices with parameters specified in Table 1. After introducing $t_{\max} = 2/\|\mathscr{A}_{[i]}\|_\infty$, one can define the time-ratio $\omega := t/t_{\max}$ so that for $\omega \in [0,1]$ the convergence of the norm bound is guaranteed (see the Appendix). By varying one of the parameters while fixing the others, and by choosing the maximum Taylor order to $\eta = 10$, the plots in Fig. 5 are obtained. It can be seen that the only dominant parameter is the time ratio $\omega$, while all other variations return norm ratios of around 1.2 which is mainly caused by choosing $\omega = 0.2$.

**Table 1** Error norm evaluation: Random matrix set generation parameters

| dimension $n$ | center-delta ratio $\sigma$ | time ratio $\omega$ | non-zero ratio $\mu$ |
|---|---|---|---|
| 20 | 3 | 0.2 | 0.3 |

### 4.5.4 Volume Evaluation

Since the performance of the matrix zonotope computations could not be evaluated in the previous norm test, we now evaluate how big the volume of the set of state transition matrices $\overline{\mathscr{M}}(t)$ is when it is computed by matrix zonotopes or interval matrices. The volume of $\overline{\mathscr{M}}(t)$ is computed by transforming it to a set in the vector space, so that interval matrices become multidimensional intervals and matrix zono-
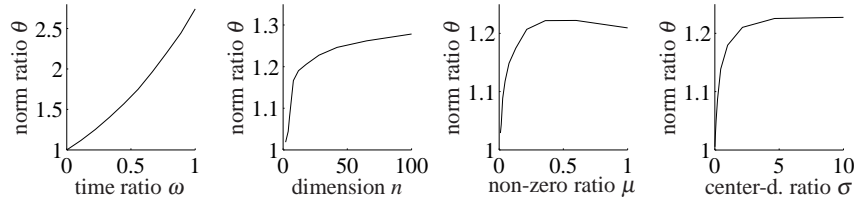
**Fig. 5** Norm evaluation: Norm ratios $\theta$ for variations of parameters while fixing the other parameters given in Table 1

topes become zonotopes. The transformation is established by stacking the column vectors of a matrix $\mathbf{Y} \in \mathbb{R}^{n \times n}$ into a vector $\mathbf{y} \in \mathbb{R}^{n^2}$.

The volume computation of multidimensional intervals is simply the product of the interval lengths in each dimension. The volume computation of a zonotope is more elaborate and $\sharp P$-hard; see [38]. For this reason, zonotopes are overapproximated by parallelotopes according to [5] for which the volume computation is much easier, meaning that the exact volume ratio is better for matrix zonotopes than shown in Fig. 6. In order to ensure that the volume is always greater than 0, the non-zero ratio $\mu$ is chosen to 1. Due to the computational load, the dimension is chosen as $n = 6$ in contrast to Table 1. For a comparison of the results, the average ratio for each dimension is computed: $\upsilon = (V_1/V_2)^{1/n^2}$, where $V_1$ is the volume of the zonotope computation, $V_2$ the volume of the interval computation, and the dimension due to the vector space transformation is $n^2$. It can be seen that especially for problems in higher dimension, matrix zonotopes perform better than interval matrices.
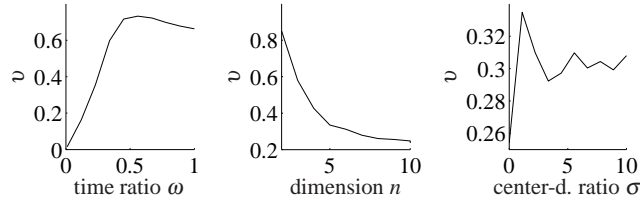


**Fig. 6** Volume evaluation: Normalized volume ratios $\upsilon$ for variations of parameters while fixing the other parameters.

# 5 Computation of Reachable Sets

As mentioned in the introduction, there exists a large number of possible representations for reachable sets. It has been shown that zonotopes and support functions outperform other representations when computing the reachable set of linear time

invariant systems [16, 39]. However, for linear systems with uncertain parameters, no efficient method has yet been proposed using support functions. Thus, zonotopes are used for the numerical examples, which are specified as in (8), except that the matrix generators are replaced by vector generators. The order of a zonotope is also defined as $\rho = \kappa/n$, where $\kappa$ is the number of generators and $n$ is the system dimension.

In order to execute Alg. 1, it remains to specify how to multiply an interval matrix or a matrix zonotope with a zonotope, and how to add zonotopes. Due to space limitations, the derivation of these operations is left to [27]. It is noted that the multiplication and addition operation can be implemented efficiently which is reflected in the numerical examples presented below.

### 5.1 Five-Dimensional Example

As a first example, the reachable set of the linear system $\dot{\mathbf{x}} = \mathbf{A}\mathbf{x} + \mathbf{u}(t)$ is computed, where $\mathbf{A} \in \mathscr{A}_{[z]}$ as specified in (12). Alternatively, the reachable set is computed with interval matrices so that $A \in \mathscr{A}_{[i]}$ as specified in (13) to compare the accuracy with the more complex matrix zonotope computations. The set of inputs is bounded by the interval $[-0.1, 0.1]$ for each dimension. The maximum order of Taylor terms is chosen to $\eta = 4$, the maximum zonotope order is chosen as $\rho = 20$, the time increment is $r = 0.05$ and the time horizon is $t_f = 5$.
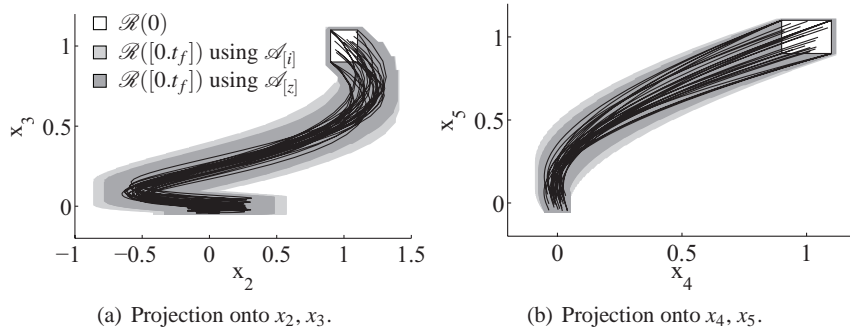


(a) Projection onto $x_2, x_3$.          (b) Projection onto $x_4, x_5$.

**Fig. 7** Reachable set of the five-dimensional example. The light gray region shows the reachable set when computing with the interval matrix $\mathscr{A}_{[i]}$, while the dark gray region shows the result when computing with the original matrix zonotope $\mathscr{A}_{[z]}$. Black lines show exemplary trajectories and the white region is the initial set

The scalability of the algorithm is shown by computing reachable sets for several randomly generated linear systems using the same parameters as for the five-dimensional system. There are no further constraints on the generation of random matrix sets, such that the sets might contain stable and/or unstable matrices. Compu-

tation times for system matrices bounded by interval matrices and matrix zonotopes are shown in Table 2. The computations have been performed in MATLAB on an Intel i7 Processor with 1.6 GHz and 6 GB memory.

**Table 2** Computation times

| Dimension $n$ | 5 | 10 | 20 | 50 | 100 |
|---|---|---|---|---|---|
| *Interval matrix* | | | | | |
| CPU time in [s] | 0.14 | 0.17 | 0.46 | 1.05 | 3.63 |
| *Matrix zonotope: Nr of generator matrices $\kappa = 1$* | | | | | |
| CPU time in [s] | 0.14 | 0.15 | 0.46 | 1.36 | 6.24 |
| *Matrix zonotope: Nr of generator matrices $\kappa = 2$* | | | | | |
| CPU time in [s] | 0.15 | 0.20 | 0.72 | 3.53 | 11.01 |
| *Matrix zonotope: Nr of generator matrices $\kappa = 4$* | | | | | |
| CPU time in [s] | 0.22 | 0.36 | 1.47 | 7.58 | 28.33 |

### 5.2 Transmission Line

The second example is a transmission line which is modeled as an R-L-C circuit, see Fig. 8. Those models are used in, e.g., timing verification of integrated circuit design [40]. Possible verification tasks are to guarantee a minimum time to reach a certain output voltage or to guarantee that a maximum output voltage is not overshot. Similar examples have been studied in [16, 41], where wrapping-free algorithms could be applied. This is not possible in this work since uncertain parameters are considered. The wrapping effect plays a dominant role in this example since the system is poorly damped, where the smallest damping ratio of all poles is 0.016. Thus, even a small wrapping effect can cause unstable reachable set computations. This effect could be decreased by applying subdivision strategies for the uncertain parameters, which would increase the computation time, however.
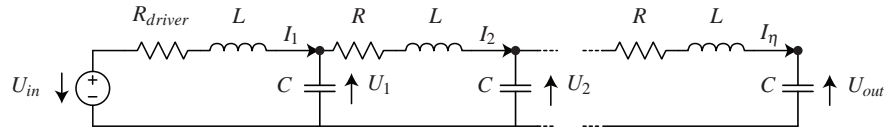


**Fig. 8** Transmission line modeled as an R-L-C circuit

After denoting the voltage and the current at the $l^{th}$ node by $U_l$ and $I_l$, respectively, and all resistances, inductances, and capacitances by $R$, $L$, $C$, the differential equations are

| first node ($l = 1$) | other nodes | last node ($l = \eta$) |
|---|---|---|
| $\dot{U}_1 = \frac{1}{C}(I_2 - I_1)$ | $\dot{U}_l = \frac{1}{C}(I_{l+1} - I_l)$ | $\dot{U}_\eta = -\frac{1}{C}I_\eta$ |
| $\dot{I}_1 = \frac{1}{L}(U_1 + U_{in}) - \frac{R_{driver}}{L}I_1$ | $\dot{I}_l = \frac{1}{L}(U_l - U_{l-1}) - \frac{R}{L}I_l$ | $\dot{I}_\eta = \frac{1}{L}(U_\eta - U_{\eta-1}) - \frac{R}{L}I_\eta$ |

$$(14)$$

with parameter ranges listed in Table 3. After introducing the state vector $\mathbf{x} = [U_1, \ldots, U_\eta, I_1, \ldots, I_\eta]^T$, the input $u = U_{in}$, and grouping the terms in (14), one can formulate the differential inclusion

$$\dot{\mathbf{x}} \in (\underbrace{[p_1]\mathbf{Q}^{(1)} + [p_2]\mathbf{Q}^{(2)} + [p_3]\mathbf{Q}^{(3)} + [p_4]\mathbf{Q}^{(4)}}_{=\mathscr{A}_{[z]}})\mathbf{x} + \underbrace{[p_1]\mathbf{r}}_{=\mathscr{B}_{[z]}}u, \qquad (15)$$

where $\mathbf{Q}^{(i)} \in \mathbb{R}^{n \times n}$, $\mathbf{r} \in \mathbb{R}^n$, and

$$[p_1] = \frac{1}{[L]}, \quad [p_2] = \frac{1}{[C]}, \quad [p_3] = \frac{[R_{driver}]}{[L]}, \quad [p_4] = \frac{[R]}{[L]}.$$

The formulation in (15) makes it possible to obtain the generators $\mathbf{G}^{(i)}$ of the matrix zonotope $\mathscr{A}_{[z]}$ as
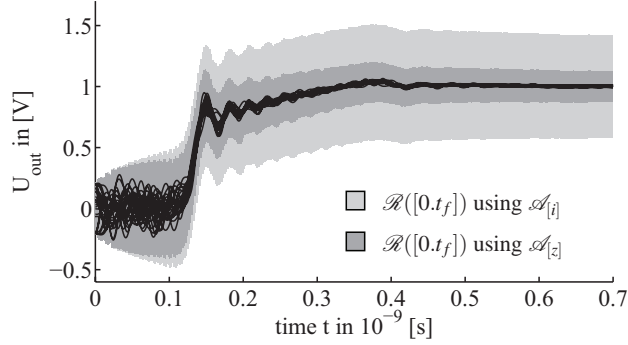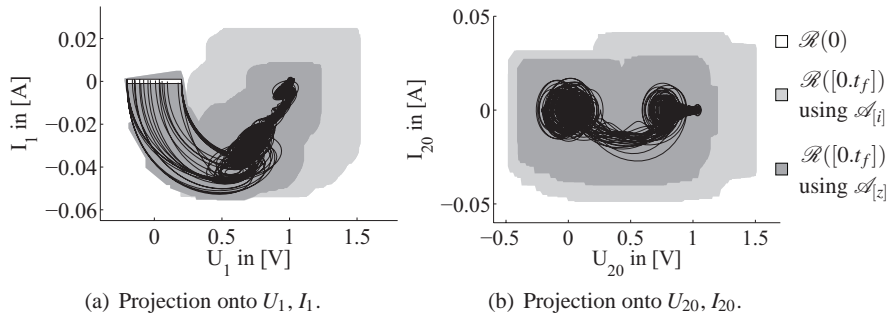
$$\mathbf{G}^{(0)} = \sum_{i=1}^{4} \mathtt{mid}\{[p_i]\}\mathbf{Q}^{(i)}, \text{ for } i = 1..4 : \mathbf{G}^{(i)} = \mathtt{rad}\{[p_i]\}\mathbf{Q}^{(i)}$$

and analogously for $\mathscr{B}_{[z]}$, where $\mathtt{mid}\{.\}$ returns the midpoint and $\mathtt{rad}\{.\}$ the radius of an interval. The initial state of the system is determined by the steady state solution for input voltages $U_{in} = u \in [-0.2, 0.2]$ to which an uncertainty is added so that the initial currents are also uncertain: $R(0) = -\mathbf{A}^{-1}\mathbf{b}u + \square(0.001)$, where $\mathbf{A}$, $\mathbf{b}$ are chosen as the matrix centers of $\mathscr{A}_{[z]}$, $\mathscr{B}_{[z]}$, and $\square(0.001)$ is a box of edge length $2 \cdot 0.001$. At time $t = 0$, the input is changed to $u \in [0.99, 1.01]$ so that the step response of the output voltage $U_{out} = U_l$ can be verified. For the modeling of the transmission line, 20 nodes have been used such that the system has 40 state variables. The reachable set of $U_{out}$ is presented in Fig. 9 when computing with matrix zonotopes (dark gray) or interval matrices (light gray). It can be observed that the matrix zonotope computations are much tighter due to the consideration of the dependency of the $R$, $L$, and $C$ values of each node. Further projections of reachable sets in the phase space are shown in Fig. 10.

The step size of the example is $r = 0.002$, the time horizon is $t_f = 0.7$, Taylor terms are computed up to order $\eta = 6$, and the maximum zonotope order is $\rho = 400$, where the order reduction is performed as in [14]. The computation time was 388 s for the matrix zonotope computation and 37 s for the interval matrix computation in MATLAB (without using the parallel computing toolbox) on an Intel i7 Processor with 1.6 GHz and 6 GB memory. Interval computations have been performed using the Matlab toolbox IntLab [42].

**Table 3** Transmission Line Parameters

| resistance in [$\Omega$] | driver resistance in [$\Omega$] | inductance in [H] | capacitance in [F] |
|---|---|---|---|
| $R \in [0.99, 1.01]$ | $R_{driver} \in [9.9, 10.1]$ | $L = 1e - 10$ | $C \in 1e - 13 \cdot [3.99, 4.01]$ |



**Fig. 9** Output voltage range of the transmission line over time. The light gray region shows the reachable set when computing with the interval matrix $\mathscr{A}_{[i]}$, while the dark gray region shows the result when computing with the original matrix zonotope $\mathscr{A}_{[z]}$. Black lines show exemplary trajectories



(a) Projection onto $U_1$, $I_1$.          (b) Projection onto $U_{20}$, $I_{20}$.

**Fig. 10** Reachable set of the transmission line example. The light gray region shows the reachable set when computing with the interval matrix $\mathscr{A}_{[i]}$, while the dark gray region shows the result when computing with the original matrix zonotope $\mathscr{A}_{[z]}$. Black lines show exemplary trajectories and the white region is the initial set

## 6 Conclusions

The computation of reachable sets for linear systems with uncertain time-invariant system matrices and time-varying inputs has been presented. The reachable set for points in time without any input is computed based on the set of state transition matrices, which is extended for time intervals and uncertain inputs. New methods for tightly overapproximating the set of state transition matrices by considering parameter dependencies have been developed for interval matrices and matrix zono-

topes. These methods are numerically evaluated and supplemented by an accurate norm estimation. Due to the use of zonotopes for the reachable set representation, the computational complexity grows moderately with the number of state variables compared to other approaches, such as the computation with arbitrary polytopes. The usefulness of the presented methods is demonstrated for the verification of a transmission line. Although the overapproximation of reachable sets is small for the first time intervals, the wrapping effect might become a dominant source for overapproximation when the system is poorly damped.

As previously mentioned, it is assumed that the implementation of the presented methods returns exact numerical results, although computers have rounding errors due to a fixed number of significant digits. This can be fixed by performing all underlying numerical computations with interval arithmetics accounting for rounding errors.

Future work aims at reducing the wrapping effect by developing new order reduction techniques for zonotopes. This might be achieved by adopting techniques used for the reduction of the wrapping effect of multidimensional intervals, such as the QR-preconditioning algorithm [29]. Preconditioning the state equations such as using the classical diagonalization of system matrices, where $\mathscr{A}^* = S \mathscr{A} S^{-1}$ and $S$ contains the eigenvectors of the nominal system matrix $\mathbf{A}_{[n]}$, has not been beneficial since the uncertainty of $\mathscr{A}^*$ is increased compared to $\mathscr{A}$ due to the necessary matrix set multiplications. However, if one could compute the range of eigenvalues and eigenvectors more efficiently and tighter as today [34], one could use these results to obtain an exactly diagonalized system matrix directly. It would then be possible to compute the set of state transition matrices for long time horizons (due to the separate evaluation for each dimension) such that wrapping-free implementation developed in [39] could be applied.

## Acknowledgements

## Appendix

## Proof of Theorem 2

The $l^{th}$ power of an interval matrix can be represented by a real valued matrix $\mathbf{C}_{[n]}(l)$ and a symmetric interval matrix $[-\mathbf{D}(l), \mathbf{D}(l)]$:

$$\mathscr{A}_{[i]}^{l} = (\mathbf{A}_{[n]} + [-\mathbf{S}, \mathbf{S}])^{l} = \mathbf{C}_{[n]}(l) + [-\mathbf{D}(l), \mathbf{D}(l)].$$

Using the nominal or center value $\mathbf{A}_{[n]}$ and the symmetric interval $[-\mathbf{S}, \mathbf{S}]$, the values of $\mathbf{C}_{[n]}(l)$ and $\mathbf{D}(l)$ can be obtained iteratively (see [31]):

$$\begin{aligned}
\mathbf{C}_{[n]}(i+1) &= \mathbf{A}_{[n]}\mathbf{C}_{[n]}(i), \\
\mathbf{D}(i+1) &\leq |\mathbf{A}_{[n]}|\mathbf{D}(i) + \mathbf{S}|\mathbf{C}_{[n]}(i)| + \mathbf{SD}(i) = (|\mathbf{A}_{[n]}| + \mathbf{S})\mathbf{D}(i) + \mathbf{S}|\mathbf{C}_{[n]}(i)|,
\end{aligned} \tag{16}$$

where $\mathbf{C}_{[n]}(1) = \mathbf{A}_{[n]}$, $\mathbf{D}(1) = \mathbf{S}$. Using this notation, the difference between the nominal exponential matrix and the overapproximated set of exponential matrices is

$$[\![e^{\mathbf{A}t}]\!]_{\mathbf{A} \in \mathscr{A}} - e^{\mathbf{A}_{[n]}t} \subseteq \sum_{i=1}^{\infty} [-\mathbf{D}(i), \mathbf{D}(i)] \frac{t^{i}}{i!}. \tag{17}$$

We are ultimately interested in $\mathbf{S}^{\Sigma}(i) := \sum_{l=1}^{i} \mathbf{D}(l) \frac{t^{l}}{l!}$ (see (17)). A matrix computation can be found for $\mathbf{S}^{\Sigma}(i)$ based on (16) when overapproximating the absolute value of $\mathbf{C}_{[n]}(i)$ by $|\mathbf{C}_{[n]}(i+1)| = |\mathbf{A}_{[n]}||\mathbf{C}_{[n]}(i)|$:

$$\begin{bmatrix} |\mathbf{C}_{[n]}(i+1)|t^{i+1} \\ \mathbf{D}(i+1)t^{i+1} \\ \mathbf{S}^{\Sigma}(i+1) \end{bmatrix} = \underbrace{\begin{bmatrix} |\mathbf{A}_{[n]}|t & 0 & 0 \\ \mathbf{S}t & (|\mathbf{A}_{[n]}| + \mathbf{S})t & 0 \\ 0 & \mathbf{I}\frac{1}{i!} & \mathbf{I} \end{bmatrix}}_{=\tilde{\mathbf{G}}(i)} \begin{bmatrix} |\mathbf{C}_{[n]}(i)|t^{i} \\ \mathbf{D}(i)t^{i} \\ \mathbf{S}^{\Sigma}(i) \end{bmatrix}.$$

In order to derive some properties from the linear update scheme, the matrix $\tilde{\mathbf{G}}(i)$ depending on $i$ is replaced by a constant matrix $\mathbf{G}$ such that the result is overapproximated. This is done by overapproximating the sum $\mathbf{S}^{\Sigma}(i) = \sum_{l=1}^{i} \mathbf{D}(l) \frac{t^{l}}{l!}$ by $\mathbf{S}^{\Sigma^{*}}(i) = \sum_{l=1}^{i} \mathbf{D}(l) \frac{t^{l}}{2^{l-1}}$:

$$\begin{bmatrix} |\mathbf{C}_{[n]}(i+1)|t^{i+1}/2^{i} \\ \mathbf{D}(i+1)t^{i+1}/2^{i} \\ \mathbf{S}^{\Sigma}(i+1) \end{bmatrix} = \underbrace{\begin{bmatrix} |\mathbf{A}_{[n]}|\frac{t}{2} & 0 & 0 \\ \mathbf{S}\frac{t}{2} & (|\mathbf{A}_{[n]}| + \mathbf{S})\frac{t}{2} & 0 \\ 0 & \mathbf{I} & \mathbf{I} \end{bmatrix}}_{=\mathbf{G}} \begin{bmatrix} |\mathbf{C}_{[n]}(i)|t^{i}/2^{i-1} \\ \mathbf{D}(i)t^{i}/2^{i-1} \\ \mathbf{S}^{\Sigma}(i) \end{bmatrix}. \tag{18}$$

When using the definition of norms of matrix sets in (3), the following relationships hold: $\|\mathbf{A}\mathbf{B}\| \leq \|\mathbf{A}\| \|\mathbf{B}\|$, $\|\mathbf{A} + \mathbf{B}\| \leq \|\mathbf{A}\| + \|\mathbf{B}\|$. The inequality for the multiplication only holds for sub-multiplicative norms, which is the case for all $p$-norms. This

makes it possible to rewrite (18) to

$$
\begin{bmatrix}
\|\mathbf{C}_{[n]}(i+1)\|t^{i+1}/2^i \\
\|\mathbf{D}(i+1)\|t^{i+1}/2^i \\
\|\mathbf{S}^{\Sigma}(i+1)\|
\end{bmatrix}
=
\underbrace{
\begin{bmatrix}
\|\mathbf{A}_{[n]}\|\frac{t}{2} & 0 & 0 \\
\|\mathbf{S}\|\frac{t}{2} & \||\mathbf{A}_{[n]}|+\mathbf{S}\|\frac{t}{2} & 0 \\
0 & 1 & 1
\end{bmatrix}}_{=\mathbf{G}_{norm}}
\begin{bmatrix}
\|\mathbf{C}_{[n]}(i)\|t^i/2^{i-1} \\
\|\mathbf{D}(i)\|t^i/2^{i-1} \\
\|\mathbf{S}^{\Sigma}(i)\|
\end{bmatrix}
$$

Due to the block-triangular structure of $\mathbf{G}_{norm}$, the eigenvalues are $\|\mathbf{A}_{[n]}\|\frac{t}{2}$, $\||\mathbf{A}_{[n]}|+\mathbf{S}\|\frac{t}{2}$, and 1. If $\||\mathbf{A}_{[n]}|+\mathbf{S}\|\frac{t}{2} < 1$, it follows that the maximum eigenvalue is 1, which is assumed from now on. Another interesting property of $\mathbf{G}_{norm}$ is that it is non-negative, i.e. $g_{norm,i,j} \geq 0$ for all $i,j = 1\ldots3$. In addition, if there exists a common natural number $m$ for all index pairs such that $(\mathbf{G}_{norm}^m)_{ij} > 0$, the matrix is not only irreducible, but primitive, too.

For primitive matrices, one can apply the Perron-Frobenius theorem that allows one to compute $\lim_{k\to\infty} \mathbf{G}_{norm}^k$ based on the left and right eigenvectors of $\mathbf{G}_{norm}$. However, due to the block-triangular structure of $\mathbf{G}_{norm}$, it follows that it is a reducible matrix and thus not primitive. In [43] it is shown that under certain conditions (see [43, Assumption 2]), the results of the Perron-Frobenius theorem can be generalized to the reducible matrix at hand, where $\mathbf{y}$ is the right and $\mathbf{q}$ the left eigenvector corresponding to the greatest eigenvalue $\bar{\lambda} = 1$: $\lim_{k\to\infty} \mathbf{G}_{norm}^k/\bar{\lambda}^k = \lim_{k\to\infty} \mathbf{G}_{norm}^k = \mathbf{yq}^T/(\mathbf{y}^T\mathbf{q})$. Using this result, and the fact that the right eigenvector is always $\mathbf{y} = \begin{bmatrix} 0 & 0 & 1 \end{bmatrix}^T$ and $q_3 = 1$, the norm of the set of matrix exponentials can be overapproximated by

$$
\|[\![e^{\mathbf{A}t}]\!]_{\mathbf{A}\in\mathscr{A}} - e^{\mathbf{A}_{[n]}t}\| \leq \underbrace{\begin{bmatrix} 0 & 0 & 1 \end{bmatrix} \frac{\mathbf{yq}^T}{\mathbf{q}^T\mathbf{y}}}_{=\mathbf{q}^T}
\begin{bmatrix}
\|\mathbf{A}_{[n]}\|t \\
\|\mathbf{S}\|t \\
0
\end{bmatrix}. \tag{19}
$$

The remaining left eigenvectors are

$$
q_1 = \frac{\|\mathbf{S}\|\frac{t}{2}}{\|\mathbf{A}_{[n]}\| \cdot \||\mathbf{A}_{[n]}|+\mathbf{S}\|\frac{t^2}{4} - (\|\mathbf{A}_{[n]}\| + \||\mathbf{A}_{[n]}|+\mathbf{S}\|)\frac{t}{2} + 1},
$$
$$
q_2 = \frac{1}{1 - \||\mathbf{A}_{[n]}|+\mathbf{S}\|\frac{t}{2}}.
$$

Inserting this result into (19) yields the result of the theorem.

## References

1. Glover, J.D., Schweppe, F.C.: Control of linear dynamic systems with set constrained disturbances. IEEE Transactions on Automatic Control **16**(5), 411–423 (1971)
2. Clarke, E., Fehnker, A., Han, Z., Krogh, B.H., Ouaknine, J., Stursberg, O., Theobald, M.: Abstraction and counterexample-guided refinement in model checking of hybrid systems. In-

ternational Journal of Foundations of Computer Science **14**(4), 583–604 (2003)

3. Schlaepfer, F.M., Schweppe, F.C.: Continuous-time state estimation under disturbances bounded by convex sets. IEEE Transactions on Automatic Control **17**(2), 197–205 (1972)

4. Althoff, M., Stursberg, O., Buss, M.: Reachability analysis of nonlinear systems with uncertain parameters using conservative linearization. In: Proc. of the 47th IEEE Conference on Decision and Control, pp. 4042–4048 (2008)

5. Althoff, M., Stursberg, O., Buss, M.: Computing reachable sets of hybrid systems using a combination of zonotopes and polytopes. Nonlinear Analysis: Hybrid Systems **4**(2), 233–249 (2010)

6. Henzinger, T.: Verification of Digital and Hybrid Systems, *NATO ASI Series F: Computer and Systems Sciences*, vol. 170, chap. The theory of hybrid automata, pp. 265–292. Springer (2000)

7. Henzinger, T.A., Ho, P.H., Wong-Toi, H.: Algorithmic analysis of nonlinear hybrid systems. IEEE Transactions on Automatic Control **43**(4), 540–554 (1998)

8. Frehse, G.: PHAVer: Algorithmic verification of hybrid systems past HyTech. In: Hybrid Systems: Computation and Control, LNCS 3413, pp. 258–273. Springer (2005)

9. Lafferriere, G., Pappas, G.J., Yovine, S.: Symbolic reachability computation for families of linear vector fields. Symbolic Computation **32**, 231–253 (2001)

10. Chutinan, A., Krogh, B.H.: Computational techniques for hybrid system verification. IEEE Transactions on Automatic Control **48**(1), 64–75 (2003)

11. Kurzhanskiy, A.B., Varaiya, P.: Ellipsoidal techniques for reachability analysis of discrete-time linear systems. IEEE Transactions on Automatic Control **52**(1), 26–38 (2007)

12. Stursberg, O., Krogh, B.H.: Efficient representation and computation of reachable sets for hybrid systems. In: Hybrid Systems: Computation and Control, LNCS 2623, pp. 482–497. Springer (2003)

13. Kühn, W.: Rigorously computed orbits of dynamical systems without the wrapping effect. Computing **61**, 47–67 (1998)

14. Girard, A.: Reachability of uncertain linear systems using zonotopes. In: Hybrid Systems: Computation and Control, LNCS 3414, pp. 291–305. Springer (2005)

15. Tomlin, C., Mitchell, I., Bayen, A., Oishi, M.: Computational techniques for the verification and control of hybrid systems. Proceedings of the IEEE **91**(7), 986–1001 (2003)

16. Girard, A., Guernic, C.L.: Efficient reachability analysis for linear systems using support functions. In: Proc. of the 17th IFAC World Congress, pp. 8966–8971 (2008)

17. Henzinger, T.A., Horowitz, B., Majumdar, R., Wong-Toi, H.: Beyond HyTech: Hybrid systems analysis using interval numerical methods. In: Hybrid Systems: Computation and Control, LNCS 1790, pp. 130–144. Springer (2000)

18. Ramdani, N., Meslem, N., Candau, Y.: Reachability analysis of uncertain nonlinear systems using guaranteed set integration. In: Proc. of the 17th IFAC World Congress, pp. 8972–8977 (2008)

19. Ramdani, N., Meslem, N., Candau, Y.: Reachability of uncertain nonlinear systems using a nonlinear hybridization. In: Hybrid Systems: Computation and Control, LNCS 4981, pp. 415–428. Springer (2008)

20. Nedialkov, N.S., Jackson, K.R.: Perspectives on Enclosure Methods, chap. A New Perspective on the Wrapping Effect in Interval Methods for Initial Value Problems for Ordinary Differential Equations, pp. 219–264. Springer-Verlag (2001)

21. Krasnochtanova, I., Rauh, A., Kletting, M., Aschemann, H., Hofer, E.P., Schoop, K.M.: Interval methods as a simulation tool for the dynamics of biological wastewater treatment processes with parameter uncertainties. Applied Mathematical Modeling **34**(3), 744–762 (2010)

22. Rauh, A., Auer, E., Hofer, E.P.: Valencia-ivp: A comparison with other initial value problem solvers. In: CD-Proc. of the 12th GAMM-IMACS International Symposium on Scientific Computing, Computer Arithmetic, and Validated Numerics. IEEE Computer Society (2007)

23. Asarin, E., Dang, T., Frehse, G., Girard, A., Le Guernic, C., Maler, O.: Recent progress in continuous and hybrid reachability analysis. In: Proc. of the 2006 IEEE Conference on Computer Aided Control Systems Design, pp. 1582–1587 (2006)

24. Prajna, S.: Barrier certificates for nonlinear model validation. Automatica **42**(1), 117–126 (2006)

25. Girard, A., Pappas, G.J.: Verification using simulation. In: Hybrid Systems: Computation and Control, LNCS 3927, pp. 272–286. Springer (2006)

26. Kapinski, J., Donzé, A., Lerda, F., Maka, H., Wagner, S., Krogh, B.H.: Control software model checking using bisimulation functions for nonlinear systems. In: Proc. of the 47th IEEE Conference on Decision and Control, pp. 4024–4029 (2008)

27. Althoff, M.: Reachability analysis and its application to the safety assessment of autonomous cars. Dissertation, TU München (2010).
URL: http://nbn-resolving.de/urn/resolver.pl?urn:nbn:de:bvb:91-diss-20100715-963752-1-4

28. Althoff, M., Le Guernic, C., Krogh, B.H.: Reachable set computation for uncertain time-varying linear systems. In: Hybrid Systems: Computation and Control (2011)

29. Lohner, R.: Perspectives on Enclosure Methods, chap. On the Ubiquity of the Wrapping Effect in the Computation of the Error Bounds, pp. 201–217. Springer (2001)

30. Dang, T.: Vérification et synthèse des systèmes hybrides. Ph.D. thesis, Institut National Polytechnique de Grenoble (2000)

31. Rump, S.M.: Fast and parallel interval arithmetic. BIT Numerical Mathematics **39**(3), 534–554 (1999)

32. Moler, C., Loan, C.V.: Nineteen dubious ways to compute the exponential of a matrix, twenty-five years later. SIAM Review **45**(1), 3–49 (2003)

33. Coxson, G.E.: Computing exact bounds on elements of an inverse interval matrix is NP-hard. Reliable Computing **5**(2), 137–142 (1999)

34. Kolev, L.V.: Outer interval solution of the eigenvalue problem under general form parametric dependencies. Reliable Computing **12**(2), 121–140 (2006)

35. Rugh, W.J.: Linear System Theory. Prentice Hall (1996)

36. Kosheleva, O., Kreinovich, V., Mayer, G., Nguyen, H.T.: Computing the cube of an interval matrix is NP-hard. In: Proc. of the ACM symposium on Applied computing, pp. 1449–1453 (2005)

37. Ahn, H.S., Chen, Y.Q., Moore, K.L.: Maximum singular value and power of an interval matrix. In: Proc. of the 2006 IEEE International Conference on Mechatronics and Automation, pp. 678–683 (2006)

38. Dyer, M., Gritzmann, P., Hufnagel, A.: On the complexity of computing mixed volumes. SIAM Journal on Computing **27**(2), 356–400 (1998)

39. Girard, A., Guernic, C.L., Maler, O.: Efficient computation of reachable sets of linear time-invariant systems with inputs. In: Hybrid Systems: Computation and Control, LNCS 3927, pp. 257–271. Springer (2006)

40. Pillage, L.T., Rohrer, R.A.: Asymptotic waveform evaluation for timing analysis. IEEE Transactions on Computer-Aided Design **9**(4), 352–366 (1990)

41. Han, Z.: Reachability analysis of continuous dynamic systems using dimension reduction and decomposition. Ph.D. thesis, Carnegie Mellon University, Electrical and Computer Engineering Department (2005)

42. Rump, S.M.: Developments in Reliable Computing, chap. INTLAB - INTerval LABoratory, pp. 77–104. Kluwer Academic Publishers (1999)

43. Dietzenbacher, E.: A limiting property for the powers of a non-negative, reducible matrix. Structural Change and Economic Dynamics **4**, 353–366 (1993)